Magnonic crystal wave guide with large spin-wave propagation velocity in CoFeB

T. Schwarze and D. Grundler[a)]
Physik Department, Lehrstuhl für Physik funktionaler Schichtsysteme, Technische Universität München, James-Franck-Str. 1, D-85747 Garching b. München, Germany

(Received 13 April 2013; accepted 22 May 2013; published online 7 June 2013)

Propagating spin-wave spectroscopy is reported for two-dimensional CoFeB antidot lattices (ADLs) with perpendicular-to-plane magnetization. The magnonic crystals consist of square lattices of 190 nm diameter holes with different periods p. At $p = 600$ nm, the velocity v_g of long wavelength spin-waves is reduced compared to the unpatterned reference film by up to about 30%. However, a large v_g is regained when we leave out a column of nanoholes in the ADLs. Such a magnonic crystal wave guide is found to support faster spin waves than a CoFeB stripe of the same geometrical width, making the finding interesting for spin-wave guiding in integrated magnonics. © *2013 AIP Publishing LLC*. [http://dx.doi.org/10.1063/1.4809757]

The research field of magnonics has attracted a lot of interest in recent years promoted by the need for miniaturization and low-power consumption in modern information technology (IT).[1] Magnonic crystals (MCs), i.e., periodically patterned ferromagnets, are the analogues of photonic crystals that are exploited in IT for the manipulation of light waves.[2] In general, spin-wave based MCs can be realized in a smaller size compared to photonic crystals and hold great promise for down-scaling microwave devices operated in the GHz frequency regime.[3,4] One of the important building blocks of future magnonic devices are integrated spin-wave wave guides.[1,5] Ferromagnetic stripes with in-plane magnetization have already been explored as wave guides.[6–10] Nanostructured wave guides or MCs with perpendicular-to-plane magnetization have not yet been studied extensively[11,12] though the relevant magnetostatic forward volume wave (MSFVW) offers advantages due to small spin-wave damping and isotropic spin-wave dispersion relations.[13] For example, a complete band gap was predicted for a MC formed by a permalloy $Ni_{80}Fe_{20}$ antidot lattice (ADL) making use of MSFVW.[12] For ADLs[14] and further magnonic applications,[3,4] CoFeB is, in particular, interesting in that spin waves exhibit a large velocity v_g and low damping.[15] At the same time, CoFeB is utilized in spin-transfer torque (STT) nanodevices[16] which in the future might serve as efficient spin wave emitters for CoFeB-based devices following Ref. 17 where a perpendicular-to-plane magnetization was studied. In this letter, we explore propagating MSFVWs in ADL-based MCs (Fig. 1) prepared from CoFeB of Ref. 15. We find a reduction of v_g when decreasing the period p of the square lattice of nanoholes (diameter of 190 nm) to a value of $p = 600$ nm. Introducing line defects,[5,18] we regain a large v_g in the corresponding channels. To avoid the large perpendicular magnetic field applied to the magnetically isotropic material of this work, thin CoFeB or a further material might be used which offer built-in perpendicular magnetic anisotropy and small spin-wave damping at the same time such as Ni/Co multilayers investigated very recently.[19] Our findings substantiate the advanced functionality of MCs for nanomagnonic applications and spin-wave guiding.[3]

In the experiments, we performed propagating spin-wave spectroscopy[6,9] using two collinear coplanar wave guides (CPWs) in perpendicular-to-plane magnetic fields H [Fig. 1(a)]. The magnetic samples were prepared by sputtering CoFeB and direct patterning of square arrays of holes using focused ion beam (FIB) etching [Fig. 1(b)]. The CoFeB mesas had a thickness d of 41 nm. The investigated ADLs had different lattice periods p, whereas the hole diameter was held constant at 190 ± 10 nm. In one sample with a period of $p = 600 \pm 10$ nm, we omitted the FIB exposure of one column of nanoholes every 20 columns [Fig. 1(c)]. This way we created line defects extending from one to the other CPW. Following the results presented later, we call a defect line "magnonic crystal wave guide (MCWG)." The separation between MCWGs was chosen to be 12 μm to avoid dipolar coupling between them. We covered the ADLs by a 5 nm thick insulating layer of Al_2O_3 using atomic layer deposition. CPWs were prepared on top of this by optical lithography and lift-off processing of evaporated chromium and gold. The CPWs had an inner and outer conductor width of

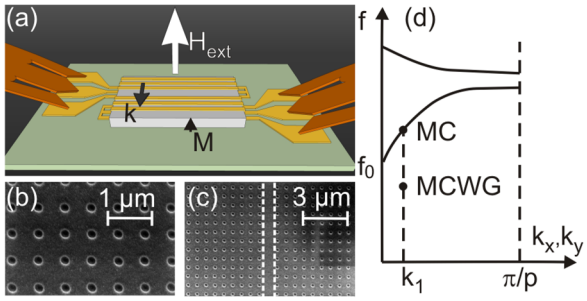

FIG. 1. (a) Schematic illustration of the spin-wave spectroscopy setup: microwave tips inject a rf current into coplanar wave guides on top of the sample (light color). The directions of the wave vector k and applied external field are depicted. Scanning electron microscopy images of an ADL (b) without and (c) with a magnonic crystal wave guide. The hole diameter (period) is 190 nm (600 nm). The white dashed lines indicate the geometrical width of the MCWG of 1020 nm. (d) Sketch of the band structure for MSFVWs in a square-lattice MC.

[a)]grundler@ph.tum.de

 © 2013 AIP Publishing LLC

2 μm with a 1.6 μm wide gap in between. The calculated distribution of wave vectors k provided a large excitation strength at $k_1 = 0.6\,10^4$ rad/cm and a smaller one at $k_2 = 2.5\,10^4$ rad/cm. The separation between inner conductor lines was $s = 12\,\mu$m. The CPWs were connected to a broadband Vector Network Analyzer (VNA) allowing us to generate a rf current with frequencies ranging from 10 MHz to 26 GHz. The accompanying rf magnetic field exerted a torque on the spins provoking spin-precessional motion with wave vectors distributed around k_1 and k_2. Later on, we will focus on excitations around k_1 corresponding to a wavelength of 10.5 μm. Resonance frequencies f were determined from spectra taken in reflection configuration on one of the CPWs. Group velocities v_g were evaluated from real and imaginary parts of spectra $\Delta S21$ obtained in transmission configuration where numbers denote the CPW. For transmissions, one CPW (CPW1) was used as an emitter and the other one (CPW2) as a detector. $\Delta S = S(H) - S(\mathrm{Ref})$ is the difference between the scattering parameter $S(H)$ measured at a given field H and $S(\mathrm{Ref})$ measured at a reference field. From the 2π phase shifts observed in $\Delta S21$, we extracted v_g following Refs. 6, 9, and 15 as detailed later. A superconducting magnet supplied fields H up to 2.5 T in a perpendicular-to-plane direction. Thereby, we addressed MSFVWs. For our discussion, we present in Fig. 1(d) a schematic band diagram with the first two bands of a nanostructured ADL assuming MSFVWs.[12] Micromagnetic simulations have been performed for plain films and ADLs considering material parameters of CoFeB such as saturation magnetization $M_s = 1430$ kA/m, a surface anisotropy constant $K_S = 37\,\mathrm{Jm}^{-2}$. The gyromagnetic ratio amounted to $\gamma/(2\pi) = 28$ GHz/T. For the ADL incorporating MCWGs, the simulation geometry was made up of a 20×20 array of holes in the xy-plane, where one column was missing. This geometry was then subdivided in 1000×1000 pixels, i.e., the lateral simulation cell size was 12 nm, being somewhat larger than the exchange length of about 5.1 nm extracted from the exchange constant of $2.75\,10^{-11}$ J/m. Two-dimensional periodic boundary conditions were applied. We needed to consider the large array in order to decouple neighboring MCWGs. The excitation was done by a spatially uniform field pulse.

In Fig. 2(a), we show the field dependencies of resonance frequencies f measured on different ADLs with periods $400\,\mathrm{nm} \le p \le 800\,\mathrm{nm}$. From sample to sample, f increases with decreasing p for a fixed field value H. Each ADL exhibits larger eigenfrequencies compared to f measured on the unpatterned reference film. The field regime depicted in Fig. 2(a) is beyond the shape anisotropy field of the unpatterned film which is about 1.6 T. As a consequence, the eigenfrequencies f of each sample exhibit an almost linear dependence on H, indicating the alignment of spins with the field direction. The observed variation of f with p is consistent with simulations[12] and experiments reported by Bali *et al.*[11] on permalloy ADLs in perpendicular-to-plane fields. It might be explained by different out-of-plane demagnetization factors which decrease with decreasing period p.

It is now interesting to study spin-wave group velocities v_g for ADLs of different p and compare them to the plain-film value. Spectra $\Delta S21$ exhibited an oscillatory behavior

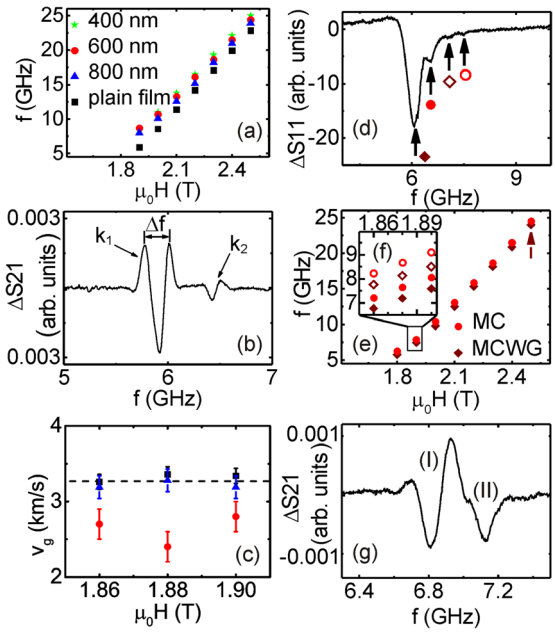

FIG. 2. (a) Resonance frequencies at k_1 measured in reflection configuration on the plain film (black squares) and ADLs (light symbols) with different p defined in the inset. (b) Transmission signal $\Delta S21$ obtained at 1.9 T on the plain film showing oscillatory signals near $f(k_1)$ and $f(k_2)$. (c) Velocities v_g measured (symbols) and calculated on the basis of Eq. (1) (dashed line) for different ALDs and the plain film, respectively, near k_1 [same symbols as in (a)]. (d) Multiple resonances (arrows) of an ADL with MCWGs at 1.82 T. Filled and open symbols stand for excitations at k_1 and k_2, respectively. Field dependencies of (e) the two most pronounced modes [mode (I) and mode (II)] and (f) all four resonances at small H seen in (d). (g) Transmission signal measured for modes (I) and (II) of the ADL with MCWGs at 1.88 T.

near $f(k_1)$ (and $f(k_2)$) as shown for the plain film at 1.9 T in Fig. 2(b). Here, we define the frequency interval Δf which indicates a phase shift of 2π in $\Delta S21$ due to propagating spin waves.[6,9,20] Using $v_g = s\Delta f$, we extract velocities for different samples as summarized in Fig. 2(c). The plain film and the ADL with $p = 800$ nm show similar v_g. We also plot calculated group velocities for the plain film as a dashed line. These values were extracted from the slope of the dispersion relation calculated according to Ref. 21

$$\omega_{\mathrm{MSFVW}}^2 = \omega_H \left[\omega_H + \omega_M \left(1 - \frac{1 - e^{-k_{||} d}}{k_{||} d} \right) \right], \qquad (1)$$

with $\omega_M = \gamma \mu_0 M_s$ and $\omega_H = \gamma \mu_0 H_{\mathrm{eff}}$, μ_0 is the permeability of vacuum, and H_{eff} is the effective field that contains the applied external field H, the static dipolar field $H_d = -M_s$ for an infinitely large thin film, and an out-of-plane field. For the calculation, we used $k_{||} = k_1$ and values for CoFeB. The measured and predicted velocities for the thin film agree well. At the same time, we see from Fig. 2(c) that the group velocity measured on the ADL with $p = 600$ nm is considerably reduced (by up to about 30%). This observation is consistent with simulations where v_g is found to decrease with decreasing p (not shown).

We now explore eigenfrequencies and group velocities of the ADL with $p = 600$ nm incorporating MCWGs. Each MCWG is formed by a missing column of nanoholes as described above. In Fig. 2(d), we show a spectrum $\Delta S11$

measured in reflection configuration at 1.82 T. We indicate four resonant features of different signal strength by black upward arrows. In Figs. 2(e) and 2(f), we plot the field dependencies of the resonances. Again, almost linear dependencies are found. Considering the two wave vectors k_1 and k_2 at which CPW1 prominently excites spin-precessional motion, the four resonances are grouped into two pairs attributed to the two different sub-components of the magnetic sample, i.e., the ADL and the nominally identical MCWGs. Comparing the data of Fig. 2(e) with Fig. 2(a), we attribute the branch with the smallest eigenfrequency [mode (I)] to the MCWGs excited at wave vector k_1. For the MCWGs, the demagnetization factor, i.e., the demagnetization field counteracting the applied field, is larger compared to the surrounding ADL. At a fixed value H, this effect leads to a smaller internal field provoking a smaller eigenfrequency for the MCWGs. Consequently, the oscillating signal near 6.8 GHz in the transmission data $\Delta S21$ of Fig. 2(g) reflects propagation in mode (I) of the MCWGs. At 1.9 T, the extracted velocity amounts to $v_g = 3.0 \pm 0.2$ km/s. The next higher lying resonance frequency in Fig. 2(e) is attributed to the ADL excited at k_1 [mode (II)]. The two further modes [open symbols in (d) and (f)] correspond to excitations in the two different sub-components at wave vector k_2.

In the following, we are interested in the profiles of mode (I) and mode (II). The simulations were performed at 2.5 T [arrow in Fig. 2(e)] far beyond the demagnetization field when spins were all aligned with H. We compare simulated (line) and measured (symbols) resonances in Fig. 3(a).[22] The simulations predict well the frequency separation between modes (I) and (II). Considering the different wave vectors for the simulation ($k = 0$) and the experiment ($k = k_1$), the one-to-one correspondence of simulated and measured eigenfrequencies f points towards a systematic but small error in the simulation.[23] The simulated spin-precessional amplitudes for modes (I) and (II) are shown in Figs. 3(b) and 3(c), respectively. Consistent with our earlier analysis, mode (I) is formed in the MCWG. Mode (II) is complementary and exists in the ADL. The MCWG mode thus lies below the eigenfrequency of the MC. This agrees to the situation in so-called index guided modes in photonic crystal wave guides.[2,24] Our further analysis shows that mode (I) is even below the MC eigenfrequency f_0 at $k = 0$, i.e., fully below the first band of the MC as sketched in Fig. 1(d). This is different to the photonic crystal where the band edge of the bottom-most allowed band at $k = 0$ is always below the index-guided mode. In magnetophotonic crystals, the optical analogue of a Tamm state has been observed showing up as an additional mid-gap resonance. The state is localized at the inner surface of the periodically patterned material and does not propagate.[25] These characteristics are also in contrast to the propagating mode that we observe.

The geometrical width of the MCWG is the edge-to-edge separation of holes which amounts to 1020 nm in the experiment [see white dashed lines in Fig. 1(c)]. We now compare the measured group velocity of about 3 km/s with values v_g of an individual CoFeB stripe acting as a magnonic wave guide. For this, we perform micromagnetic simulations on a device shown in Fig. 4(a). The total length (width) is $l_1 = 65.28\,\mu$m ($w_1 = 2040$ nm). The magnetic material takes up half of the simulation width, i.e., $w_2 = 1020$ nm, illustrated by the dark gray color. The whole device is subdivided into 128×4096 pixels and two-dimensional periodic boundary conditions are applied. In order to get the dispersion relation, we excite spin waves using a spatially confined short field pulse. After a two-dimensional fast Fourier transformation, we get the dispersion relation[26] and extract the group velocity in the limit of small wave vectors using a linear fit. For $w_2 = 1020$ nm and $\mu_0 H = 1.9$ T, we obtain $v_g = 1.9 \pm 0.2$ km/s. Due to confinement, the stripe thus supports substantially slower spin waves compared to the MCWG (slower by about 30%). To check the outcome of the simulation, we also considered $w_2 = w_1$, i.e., we modelled the plain film. Here, we extracted a group velocity of $v_g = 3.3 \pm 0.2$ km/s. This value was in good agreement with the calculated group velocity of $v_g = 3.3$ km/s using Eq. (1), substantiating the reliability of the micromagnetic approach. In Fig. 4(b), we summarize measured and simulated values v_g obtained on the three samples for comparison. The data show that v_g of the MCWG found near 1.9 T is close to the value of the unpatterned thin film and considerably larger than the stripe of the same geometrical width.

A detailed inspection of the simulated mode profile in Fig. 3(b) tells us that mode (I) is not localized perfectly within the column of missing holes. A non-zero spin-precessional amplitude exists also in the ADL. Mode (I) thus experiences an effective width w_{eff} which is larger than the geometrical one. The effective width for individual ferromagnetic stripes was introduced by Guslienko *et al.* in Ref. 27. In order to explain eigenfrequencies of laterally confined modes an effective "pinning" parameter η was defined according to $\eta(p) = 2\pi/(p[1 + 2\ln(1/p)])$ with p being the aspect ratio of the stripe ($p = \mathrm{length}/\mathrm{width}$). This parameter can be rewritten as $w_{\mathrm{eff}} = w[\eta/(\eta - 2)]$ which gives $w_{\mathrm{eff}} = 1180$ nm for the stripe with $w = 1020$ nm. w_{eff} is larger than w by 15% and

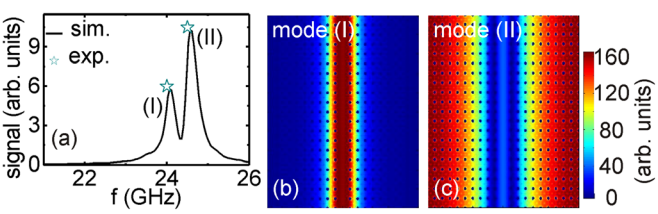

FIG. 3. (a) Simulated spectrum (line) and experimental data (stars) of the ADL with MCWGs at 2.5 T. Spin-precessional amplitudes as simulated for (b) mode (I) and (c) mode (II) seen in the spectrum of (a). The color code for amplitudes is shown on the right.

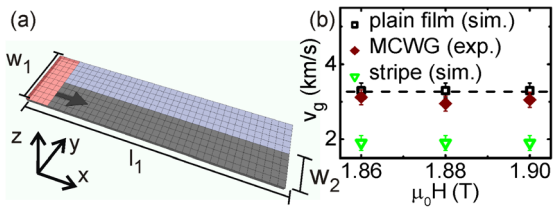

FIG. 4. (a) Geometry to simulate propagation (thick arrow) in a 41 nm thick magnetic stripe (dark gray). The light shaded area at the left end is excited by a pulse. (b) Simulated (open symbols) and experimental (filled symbols) data v_g of a plain film (squares with broken line), MCWG (diamond), and stripe (triangle).

measures the distance between nodes of the fundamental mode existing in an individual stripe. In Fig. 3(b), we see that the nodes of mode (I) in the MCWG extend much further into the MC than 15% of w_2. Wider magnetic stripes are known to support faster spin-waves than narrow ones. The large velocity v_g of the MCWG which is close to the plain film value in Fig. 4(b) is reasonable considering the large effective width illustrated in Fig. 3(b).

In summary, we studied propagating spin-waves in magnonic crystals with perpendicular-to-plane magnetization. The magnonic crystals were formed by antidot lattices of different periods p. For $p < 800$ nm, we found a reduced propagation velocity compared to the unpatterned film. A missing column of holes created a magnonic crystal wave guide which supported a fast spin wave at $p = 600$ nm. This was explained by an effective width of the mode which was much larger than the geometrical width of the wave guide itself. We showed that the MCWG is fundamentally different from the established photonic crystal wave guide in that MCWG frequencies lie below the allowed bands of the MC. Considering the isotropic dispersion relations for MSFVW, the MCWG offers new flexibility for spin wave guiding in future magnonic devices using tailored arrays of nanoholes in a ferromagnetic thin film.

We thank M. Bahr and R. Huber for experimental support. The work has received financial support from the DFG via the German Excellence Cluster "Nanosystems Iniative Munich" and the European Community's Seventh Framework Programme (FP7/2007-2013) under Grant No. 228673 (MAGNONICS).

[1]ITRS, International Technology Roadmap for Semiconductors, 2011; see http:/www.itrs.net for updates.
[2]J. D. Joannopoulos, S. G. Johnson, J. N. Winn, and R. D. Meade, *Photonic Crystals, Molding the Flow of Light* (Princeton University Press, 2008).
[3]S. Neusser and D. Grundler, Adv. Mater. **21**, 2927 (2009).
[4]V. V. Kruglyak, S. O. Demokritov, and D. Grundler, J. Phys. D: Appl. Phys. **43**, 264001 (2010).
[5]B. Lenk, H. Ulrichs, F. Garbs, and M. Münzenberg, Phys. Rep. **507**, 107 (2011).
[6]M. Bailleul, D. Olligs, C. Fermon, and S. O. Demokritov, EPL **56**, 741 (2001).
[7]S. Choi, K.-S. Lee, K. Y. Guslienko, and S.-K. Kim, Phys. Rev. Lett. **98**, 087205 (2007).
[8]V. E. Demidov, S. O. Demokritov, K. Rott, P. Krzysteczko, and G. Reiss, Appl. Phys. Lett. **92**, 232503 (2008).
[9]M. Bao, K. Wong, A. Khitun, J. Lee, Z. Hao, K. L. Wang, D. W. Lee, and S. X. Wang, EPL **84**, 27009 (2008).
[10]K. Vogt, H. Schultheiss, S. Jain, J. E. Pearson, A. Hoffmann, S. D. Bader, and B. Hillebrands, Appl. Phys. Lett. **101**, 042410 (2012).
[11]R. Bali, M. Kostylev, D. Tripathy, A. Adeyeye, and S. Samarin, Phys. Rev. B **85**, 104414 (2012).
[12]T. Schwarze, R. Huber, G. Duerr, and D. Grundler, Phys. Rev. B **85**, 134448 (2012).
[13]D. D. Stancil and A. Prabhakar, *Spin Waves: Theory and Applications* (Springer, 2009).
[14]H. Ulrichs, B. Lenk, and M. Münzenberg, Appl. Phys. Lett. **97**, 092506 (2010).
[15]H. Yu, R. Huber, T. Schwarze, F. Brandl, T. Rapp, P. Berberich, G. Duerr, and D. Grundler, Appl. Phys. Lett. **100**, 262412 (2012).
[16]Z. Zeng, G. Finocchio, B. Zhang, P. K. Amiri, J. A. Katine, I. N. Krivorotov, Y. Huai, J. Langer, B. Azzerboni, K. L. Wang, and H. Jiang, Sci. Rep. **3**, 1426 (2013).
[17]M. Madami, S. Bonetti, G. Consolo, S. Tacchi, G. Carlotti, G. Gubbiotti, F. B. Mancoff, M. A. Yar, and J. Akerman, Nat. Nanotechnol. **6**, 635 (2011).
[18]M. Madami, G. Gubbiotti, S. Tacchi, G. Carlotti, and S. Jain, "Study of the spin excitations in antidot lattices with line defects," Physica B: Condensed Matter (to be published), available at http://www.journals.elsevier.com/physica-b-condensed-matter/.
[19]M. Haertinger, C. H. Back, S.-H. Yang, S. S. P. Parkin, and G. Woltersdorf, J. Phys. D: Appl. Phys. **46**, 175001 (2013).
[20]As CPW1 provides a wave vector $k + \Delta k$ when $f + \Delta f$ is applied by the VNA, the spin-precession-induced voltage detected at CPW2 develops a phase shift of $\Delta\Phi = \Delta k s$ depending on the spin-wave dispersion relation $f(k)$. v_g is extracted via $v_g = 2\pi\Delta f/\Delta k = s\Delta f$ when taking Δf between two neighboring maxima of $\Delta S21$ for which $\Delta\Phi = 2\pi$.
[21]B. A. Kalinikos and A. N. Slavin, J. Phys. C **19**, 7013 (1986).
[22]Simulations were performed also at lower fields, but were stable only for smaller arrays. Then, however, the separation between MCWGs was smaller, leading to dynamic coupling that shifted the eigenfrequencies.
[23]The excellent agreement between experimental and simulated resonance frequencies is fortuitous as γ of the commercial simulation program is a little bit off from CoFeB. Importantly, the frequency separation is excellently reproduced which is less affected by this.
[24]C. Jamois, R. Wehrspohn, L. Andreani, C. Hermann, O. Hess, and U. Gösele, Photonics Nanostruct. Fundam. Appl. **1**, 1 (2003).
[25]T. Goto, A. V. Dorofeenko, A. M. Merzlikin, A. V. Baryshev, A. P. Vinogradov, M. Inoue, A. A. Lisyansky, and A. B. Granovsky, Phys. Rev. Lett. **101**, 113902 (2008).
[26]V. Kruglyak and R. Hicken, J. Magn. Magn. Mater. **306**, 191 (2006).
[27]K. Guslienko, S. Demokritov, B. Hillebrands, and A. Slavin, Phys. Rev. B **66**, 132402 (2002).